Zygote **24** (February), pp. 42–47. © Cambridge University Press 2014
doi:10.1017/S0967199414000690 First Published Online 16 December 2014

Pre-meiotic transformation of germplasm-related structures during male gamete differentiation in *Xenopus laevis*

Arkadiy A. Reunov and Yulia A. Reunova
A.V. Zhirmunsky Institute of Marine Biology FEB RAS, Laboratory of Cell Differentiation, Vladivostok, Russia

Date submitted: 19.03.2014. Date revised: 29.10.2014. Date accepted: 31.10.2014

Summary

To highlight the ultrastructural features of transformation occurring with germplasm-related structures (GPRS), the spermatogenic cells of *Xenopus laevis* were studied by transmission electron microscopy and quantitative analysis. It was determined that in spermatogonia and spermatocytes, the compact germinal granules underwent fragmentation into particles comparable with inter-mitochondrial cement (IMC). Fragments of IMC agglutinated some cell mitochondria and resulted in the creation of mitochondrial clusters. Clustered mitochondria responded with loss of their membranes that occurred by the twisting of membranous protrusions around themselves until multi-layered membranes were formed. The mitochondrial affinity of multi-layered membranes was proven by an immunopositive test for mitochondrial dihydrolipoamide acetyltransferase. As a consequence of mitochondrial membrane twisting, the naked mitochondrial cores appeared and presumably underwent dispersion, which is the terminal stage of GPRS transformation. As no GPRS were observed in spermatids and sperm, it was assumed that these structures are functionally assigned to early stages of meiotic differentiation.

Keywords Germinal granules, Inter-mitochondrial cement, Mitochondria, Spermatogenesis, *Xenopus laevis*.

Introduction

The germplasm of *Xenopus laevis* consists of germinal granules that are formed during oogenesis with the participation of the Balbiani body (Kloc *et al.*, 2002; Chang *et al.*, 2004; King *et al.*, 2005). Similar to the germplasm of other animals (Eddy, 1975; Mahowald, 1977; Strome & Wood, 1982; Ikenishi, 1998), the germinal granules of *X. laevis* are incorporated into primordial germline cells that migrate through embryogenesis, locate in the gonads of new generation offspring and differentiate into either eggs or sperm depending on the sex of the gonads (Saffman & Lasko, 1999; Matova & Cooley, 2001). It is possible that the pre-meiotic role of the germplasm is similar in both sexes, but this role has been poorly investigated in *X. laevis* as well as in the other metazoan animals.

It seems likely that spermatogenesis is a better model to exactly study the pre-meiotic activity of germplasm rather than oogenesis, which is peculiar in having confusing overlap of the inherited maternal germplasm and newly forming daughter germplasm assigned for the functioning of germline cells in the next generation (Reunov, 2006). According to previous ultrastructural data obtained for *X. laevis*, in early spermatogenic cells (such as spermatogonia and primary spermatocytes) the germplasm is represented by electron-dense, cytoplasmic germinal granules of different sizes and nuage that sometimes are closely associated with mitochondria (Kalt, 1973; Kerr & Dixon, 1974). It is known that germplasm is characteristic of early meiosis and disappears around pachytene (Kerr & Dixon, 1974). However, the processes occurring prior to the disappearance of this material are not known. As reported for sea urchins and mice, the germplasm-related structures (GPRS) undergo transformation that is completed by a release

[1]All correspondence to: A.A. Reunov. Laboratory of Cell Differentiation, Paltchevsky st.-17, A.V. Zhirmunsky Institute of Marine Biology, Far East Branch of the Russian Academy of Sciences, 690041 Vladivostok, Russia. Tel: +7 4232 311143. Fax: +7 4232 310900. e-mail: arkadiy_reunov@hotmail.com
[2]A.V. Zhirmunsky Institute of Marine Biology FEB RAS, Laboratory of Cell Differentiation, Paltchevsky st.-17, Vladivostok, 690041, Russia.

of their mitochondrial contents (Reunov *et al.*, 2000; Reunov, 2006, 2013). To determine whether this pre-meiotic machinery is also characteristic for *X. laevis*, the male GPRS were analysed by electron microscopy. Quantitative analyses were done to detect all features of their ultrastructural transformation.

Materials and methods

Electron microscopy

Xenopus male gonads were dissected, cut into small pieces and fixed overnight in primary fixative containing 2.5% glutaraldehyde in 0.1 M cacodylate buffer (pH 7.5) at 4°C. Fixed pieces were washed in cacodylate buffer, postfixed in 2% OsO_4 in 0.1 M cacodylate buffer for 2 h, rinsed in 0.1 M cacodylate buffer and distilled water, dehydrated in an ethanol series and acetone, and embedded in Spurr's resin. Ultra-thin sections were mounted on slot grids coated with formvar film. Sections were stained with 2% alcoholic uranyl acetate and aqueous lead citrate before being examined with a transmission electron microscope. Ultra-thin sections were examined with a transmission electron microscope (Zeiss Libra 120).

Immunoelectron microscopy

The antibody for mitochondrial dihydrolipoamide acetyltransferase, the E2 component of the pyruvate dehydrogenase complex were generated and used for study in the laboratory of Dr K.L. Mowry (see Denegre *et al.*, 1997; Volodina *et al.*, 2003) and further were generously provided for our research. Pieces of testes were fixed in 4% paraformaldehyde and 0.5% glutaraldehyde in 0.1 M cacodylate buffer and washed three times 15 min each in phosphate-buffered saline (PBS) with 0.05% Tween 20. Fixed tissues were then blocked in casein buffer [BioRad, 1% casein in Tris-buffered saline (TBS)] overnight at room temperature, followed by overnight incubation with shaking in mouse primary anti-dihydrolipoamide acetyltransferase antibodies diluted in casein buffer (1:100). Negative controls were run by omitting the primary antibodies. Materials were further washed three times 60 min each in PBS with 0.05% Tween 20, incubated with anti-mouse nanogold (size 1.4 nm) antibodies in casein buffer (1:50), and washed again three times 60 min each in PBS with 0.05% Tween 20. Afterwards, materials were postfixed in the same fixative for 20 min, washed two times for 5 min each in PBS with 0.05% Tween 20, washed three times 10 min each in molecular grade water and enhanced with gold for 30 min (Nanoprobes, GoldEnhance EM, Catalogue no. 2131). The enhancement reaction was terminated by washing in molecular biology grade water three times 10 min, and materials were postfixed in the same fixative. Fixed testes were rinsed in cacodylate buffer and distilled water, dehydrated in an ethanol series and acetone, and then infiltrated and embedded in Spurr's resin. Ultra-thin sections were stained with 2% alcoholic uranyl acetate and aqueous lead citrate before being examined with a transmission electron microscope (Zeiss Libra 120).

Quantitative analysis

For transmission electron microscopy, three pieces of testis were taken from each of three individuals, and these pieces were embedded in resin blocks. From each of these nine blocks, three sections were taken from different levels. Thus, 27 sections were investigated. The presence and ultrastructural features of the GPRS were investigated in four cell types of successive stages of male gamete differentiation. These cell types were identified using typical ultrastructural features. Spermatogonia were identified by their adherence to the gonad wall as well as by nuclei filled with electron-dense small patches of chromatin and a large nucleolus. Primary spermatocytes were characterized by their location above spermatogonia as well as by their larger size and presence of synaptonemal complexes that signify the zygotene–pachytene stage of meiosis. Spermatids were identified at the late spermiogenesis stage by their elongated nuclei and strongly condensed chromatin. Spermatozoa were identified as long cells with completely condensed chromatin.

From each section, 15 spermatogonia, 15 primary spermatocytes, 15 spermatids and 15 sperm were used for counting. Thus, 405 cells at each of these stages were investigated, to give a total of 1620 cells. Percentages of GPRS were calculated and results were analysed statistically using Student's *t*-test.

Results and Discussion

It was found that GPRS are presented by germinal granules that were electron-dense structures lacking internal or external membranes (Fig. 1*A*). However, these granules were also found in a diffuse or nuage-like state (Fig. 1*B*, *C*). In addition, their fragments were seen in contact with mitochondria (Fig. 1*D*). Moreover, some similar materials were frequently observed between the mitochondria of mitochondrial clusters (Fig. 1*E*), and obviously act as so-called IMC or 'inter-mitochondrial cement' that usually agglutinates mitochondria in reproductive cells (see for review Chuma *et al.*, 2009). Thus, we observed the patterns of germplasm that are really comparable

https://doi.org/10.1017/S0967199414000690 Published online by Cambridge University Press

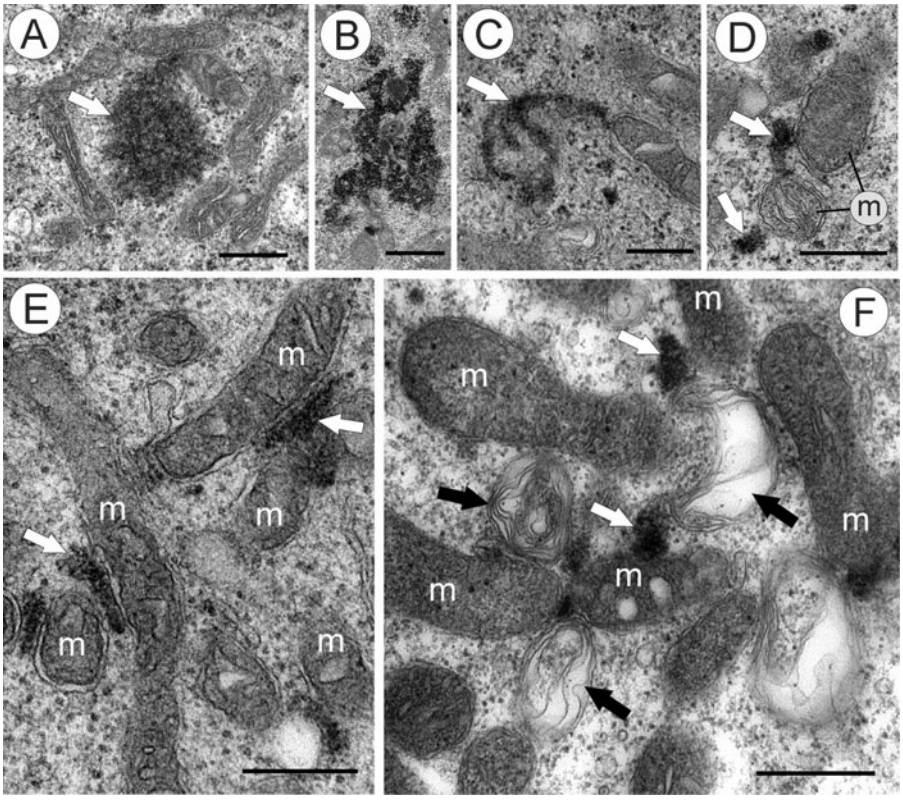

Figure 1 Patterns of GPRS in spermatogonia and primary spermatocytes of *Xenopus laevis* by transmission electron microscopy (TEM). (*A*) A compact germinal granule (arrow). (*B*, *C*) The various morphs of dispersed germinal granules (arrows). (*D*) The fragments of dispersed germinal granules (arrows) contacting mitochondria (m). (*E*) A mitochondrial cluster formed due to agglutination of mitochondria (m) by fragments of dispersed germinal granules (arrows) acting as inter-mitochondrial cement (IMC). (*F*) A mitochondrial cluster in that not only mitochondria (m) but also the multi-layered membranes (black arrows) are agglutinated by IMC (white arrows). Scale bars = 0.5 μm.

with those described in previous reports (Kalt, 1973; Kerr & Dixon, 1974). However, one more GPRS pattern was found in the course of the present study. Indeed, the mitochondrial clusters that are peculiar in having multi-layered membranes were recorded along with usual mitochondrial clusters (Fig. 1*F*). We have observed that the appearance of these multi-layered membranes occurs because the clustered mitochondria respond by altering their membranes. Such mitochondria were frequently observed with membranous protrusions (Fig. 2*A*). In many instances, these membranous projections appeared longer (Fig. 2*B*) and gradually coiled around themselves (Fig. 2*C*, *D*). It was frequently observed that multi-layered membranes occupied the 'mitochondrial place' in mitochondrial clusters and contacted IMC in a similar manner (Fig. 2*E*). Immunoelectron microscopy revealed that multi-layered membranes were stained by antibodies for mitochondrial protein dihydrolipoamide acetyltransferase, the E2 component of the pyruvate dehydrogenase complex, and proves the mitochondrial affinity of these structures (Fig. 2*F*). Based on these observations, we are confident that multi-layered membranes are mitochondrial remnants that arise due to the degradation of mitochondria. To characterise this type of mitochondrial cluster, we suggest the term 'degrading mitochondrial clusters', which seems to be appropriate to show distinction from the usual mitochondrial cluster.

Thus, four patterns of GPRS such as 'compact granules', 'dispersed granules', 'mitochondrial clusters' and 'degrading mitochondrial clusters' were identified. These GPRS were found in spermatogonia and primary spermatocytes. Spermatids and sperm lacked any GPRS. Therefore, it seems likely that GPRS are involved in the early stages of sperm differentiation but have no connection with its final phase, as is consistent with the data of Kerr & Dixon (1974), who reported the disappearance of GPRS during pachytene.

Quantitative analysis revealed that the proportions of GPRS patterns vary. In spermatogonia, the GPRS consisted of 31% compact granules, 28% dispersed granules, 22% mitochondrial clusters, and 19% degrading mitochondrial clusters (Fig. 3*A*). Primary spermatocytes contained fewer compact granules

https://doi.org/10.1017/S0967199414000690 Published online by Cambridge University Press

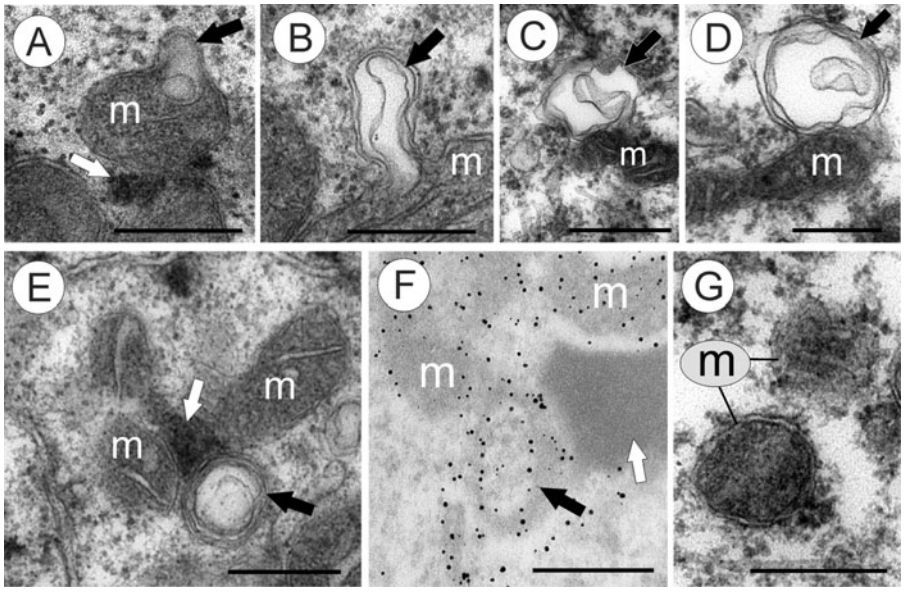

Figure 2 Alterations occurring with mitochondria clustered by inter-mitochondrial cement (IMC) in spermatogonia and primary spermatocytes of *Xenopus laevis* (TEM). (*A*) A membranous protrusion (black arrow) that appeared on the surface of mitochondria (m) contacting IMC (white arrow). (*B*) An elongated membranous protrusion (black arrow) on the surface of mitochondrion (m). (*C*, *D*) The projections (arrows) of mitochondrial membranes that undergo progressive twisting being in contact with mitochondria (m). (*E*) A mitochondrial cluster in that IMC (white arrow) agglutinates not only the mitochondria (m) but also the multi-layered membrane (black arrow) connecting to IMC in a like manner. (*F*) An IMC (white arrow) is surrounded by mitochondria (m) and multi-layered membrane (black arrow) that are both positive for mitochondrial protein dihydrolipoamide acetyltransferase. (*G*) Transverse section of two mitochondria (m) one of which has both mitochondrial membranes (bottom) and the other lacks membranes (top). Scale bars = 0.2 μm (*A*, *B*), 0.5 μm (*C*–*G*).

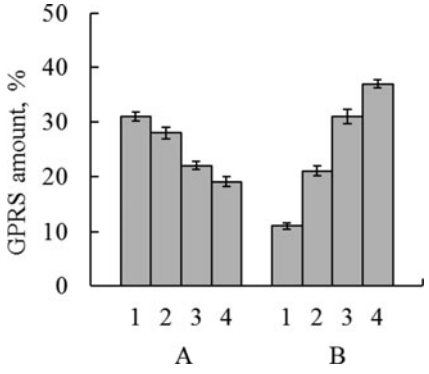

Figure 3 Diagram showing proportions of GPRS in spermatogenic cells of *Xenopus laevis*. (*A*) Spermatogonia. (*B*) Primary spermatocytes; 1, compact germinal granule; 2, dispersed germinal granule; 3, mitochondrial cluster; 4, degrading mitochondrial cluster.

(11%) and dispersed granules (21%). However, there were more mitochondrial clusters and degrading mitochondrial clusters, comprising 31 and 37%, respectively (Fig. 3*B*).

As the amount of compact granules greatly decreased during the differentiation of spermatogonium to primary spermatocytes it seemed logical that, in spermatogonia and spermatocytes, the compact granules undergo fragmentation to their dispersed form (Fig. 4*A*–*C*). The amount of dispersed granules also decreased, as they turn into IMC during the formation of mitochondrial clusters (Fig. 4*C*–*E*). Indeed, the number of mitochondrial clusters increased in spermatocytes relative to spermatogonia. Taking into account that there are more mitochondrial clusters than degrading mitochondrial clusters in spermatogonia, but that the quantity of degrading mitochondrial clusters in primary spermatocytes exceeds the amount of unchanged mitochondrial clusters, it seems logical that the appearance of mitochondria featured by the development of protruded areas of their membranes (Fig. 4*E*) followed by gradual twisting of these into multi-layered membranes (Fig. 4*F*, *G*) completes the whole cascade of interactions between germinal granules and mitochondria.

It seems likely that the cores of mitochondria become naked (Fig. 4*G*) after mitochondrial membrane twisting. Indeed, two types of mitochondria, one type surrounded by a double membrane and the other lacking any external membranes, were regularly observed in cross-sections (Fig. 2*G*). We did not observe the next transformation of naked mitochondrial cores. However, as these structures disappeared during spermatogenesis, we suggest that the mitochondrial matrix undergoes dissemination.

https://doi.org/10.1017/S0967199414000690 Published online by Cambridge University Press

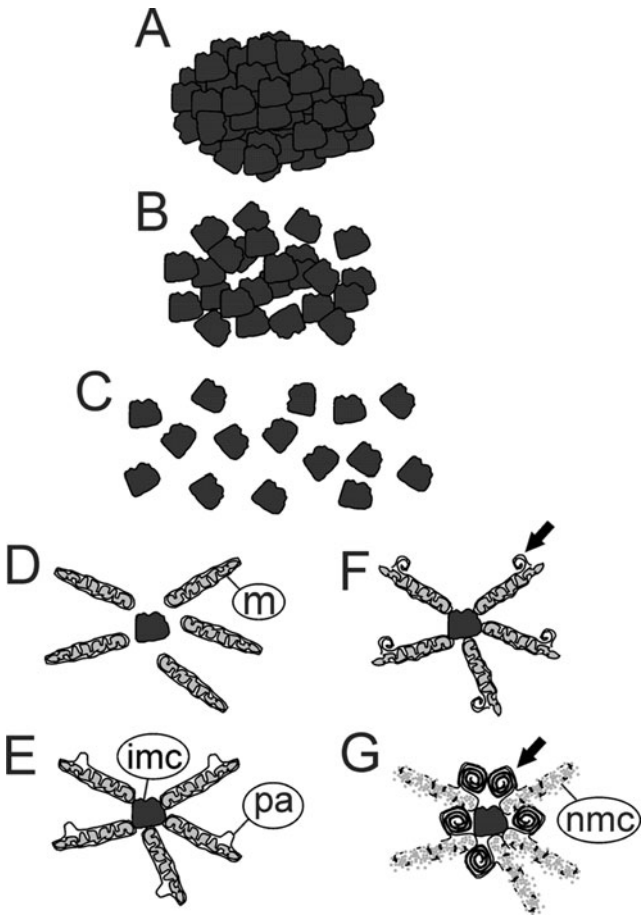

Figure 4 Schematic drawings of GPRS transformation in spermatogonia and primary spermatocytes of *Xenopus laevis*. (*A*) Compact germinal granule. (*B*, *C*) Progressive stages of compact granule dispersion followed by the appearance of relatively smaller fragments. (*D*, *E*) Progressive stages of mitochondrion (m) agglutination by germinal granule fragments acting as inter-mitochondrial cement (imc) followed by formation of a mitochondrial cluster; note the appearance of protruded areas (pa) on membranes of clustered mitochondria. (*F*, *G*) Formation of multi-layered membranes during progressive twisting of mitochondrial membranes (arrows) followed with formation of naked mitochondrial cores (nmc).

Overall, the principle of GPRS transformation provoked by germinal granules during spermatogenesis in *X. laevis* is homologous to pre-meiotic cascades previously described for mice and sea urchins, although the ultrastructural details are obviously species specific. Indeed, in mice, the mitochondria clustered by particles of fragmented germplasm do not degrade but emit membranous conglomerates (Reunov, 2006). In sea urchins, the germplasm does not undergo fragmentation, but two germplasm patterns aggregate together to form a structural centre that binds mitochondria followed by total dissemination of the formed mitochondrial clusters (Reunov, 2013). Thus, although sea urchin, frog and mouse each show characteristic differences in the pre-meiotic GPRS machinery, in all three cases, mitochondrial content is finally released into the cytoplasm.

Thereby, in the course of the present study, the mitochondrial matrix release provoked by maternal postembryonic germplasm was found in early meiotic cells of *X. laevis* males. Moreover, the same phenomenon was discovered previously during spermatogenesis in sea urchins and mice (Reunov, 2006, 2013). According to Hecht (1998) and Gur & Breitbart (2006, 2008), the loss of cell ribosomes and their replacement by mitochondrial ribosomes occurs during spermatogenesis. Thus, the penetration of the mitochondrial matrix into the cytoplasm of spermatogonia may be connected with the extra-mitochondrial localisation of mitochondrial ribosomes that are presumably able to initiate the translation of nuclear mRNAs (Amikura *et al.*, 2001, 2005; Villegas *et al.*, 2002; Thomson & Lasko, 2005). This hypothesis requires more detailed investigation in model systems.

Acknowledgements

This work was supported by the FEB RAS (grant No. 12-I-П6–08) for Dr A.A. Reunov. Part of the study was done in the Immunobiology Laboratory of The Methodist Hospital Research Institute (Houston, TX, USA). We are very grateful to Dr M. Kloc for help. Anti-dihydrolipoamide acetyltransferase antibodies were generously provided by Dr K.L. Mowry.

References

Amikura, R., Kashikawa, M., Nakamura, A. & Kobayashi, S. (2001). Presence of mitochondria-type ribosomes outside mitochondria in germ plasm of *Drosophila* embryos. *Proc. Natl. Acad. Sci. USA* **98**, 9133–8.

Amikura, R., Sato, K. & Kobayashi, S. (2005). Role of mitochondrial ribosome-dependent translation in germline formation in *Drosophila* embryos. *Mech. Develop.* **122**, 1087–93.

Chang, P., Torres, J., Lewis, R.A., Mowry, K.L., Houliston, E. & King, M.L. (2004). Localization of RNAs to the mitochondrial cloud in *Xenopus* oocytes through entrapment and association with endoplasmic reticulum. *Mol. Biol. Cell* **15**, 4669–81.

Chuma, S., Hosokawa, M., Tanaka, T. & Nakatsuji, N. (2009). Ultrastructural characterization of spermatogenesis and its evolutionary conservation in the germline: germinal granules in mammals. *Mol. Cell. Endocrinol.* **306**, 17–23.

Denegre, J.M., Ludwig, E.R. & Mowry, K.L. (1997). Localized maternal proteins in *Xenopus* revealed by subtractive immunization. *Dev. Biol.* **192**, 446–54.

https://doi.org/10.1017/S0967199414000690 Published online by Cambridge University Press

Eddy, E.M. (1975). Germ plasm and the differentiation of the germ cell line. *Int. Rev. Cytol.* **43**, 229–80.

Gur, Y. & Breitbart, H. (2006). Mammalian sperm translate nuclear-encoded proteins by mitochondrial-type ribosomes. *Genes Dev.* **20**, 411–6.

Gur, Y. & Breitbart, H. (2008). Protein synthesis in sperm: dialog between mitochondria and cytoplasm. *Mol. Cell. Endocrinol.* **282**, 45–55.

Hecht, N.B. (1998). Molecular mechanisms of male germ cell differentiation. *BioAssay* **20**, 555–61.

Ikenishi, K. (1998). Germ plasm in *Caenorhabditis elegans, Drosophila* and *Xenopus. Dev. Growth Differ.* **40**, 1–10.

Kalt, M.R. (1973). Ultrastructural observations on the germ line of *Xenopus laevis*. *Z. Zellforsch.* **138**, 41–62.

Kerr, J.B. & Dixon, K.E. (1974). An ultrastructural study of germ plasm in spermatogenesis of *Xenopus laevis*. *J. Embryol. Exp. Morph.* **32**, 573–92.

King, M.L., Messitt, T. & Mowry, K. (2005). Putting RNAs in the right place at the right time: RNA localization in the frog oocyte. *Biol. Cell* **97**, 19–33.

Kloc, M., Dougherty, M.T., Bilinski, S., Chan, A.P., Brey, E., King, M.L, Patrick, C.W. & Etkin, L.D. (2002). Three-dimensional ultrastructural analysis of RNA distribution within germinal granules of *Xenopus*. *Dev. Biol.* **241**, 79–93.

Mahowald, A.P. (1977). The germ plasm of *Drosophila:* An experimental system for the analysis of determination. *Am. Zool.* **17**, 551–63.

Matova, N. & Cooley, L. (2001). Comparative aspects of animal oogenesis. *Dev. Biol.* **231**, 291–320.

Reunov, A.A. (2006). Structures related to the germ plasm in mouse. *Zygote* **14**, 231–8.

Reunov, A.A. (2013). Premeiotic transformation of germ plasm-related structures during the sea urchin spermatogenesis. *Zygote* **27**, 95–101.

Reunov, A.A., Isaeva, V.V., Au, D.W.T. & Wu, R.S.S. (2000). Nuage constituents arising from mitochondria: is it possible? *Dev. Growth Differ.* **42**, 139–43.

Saffman, E.E. & Lasko, P. (1999). Germline development in vertebrates and invertebrates. *Cell Mol. Life Sci.* **55**, 1141–63.

Strome, S. & Wood, W.B. (1982). Immunofluorescence visualization of germ-line specific granules cytoplasmic granules in embryos, larvae and adults of *Caenorhabditis elegans*. *Proc. Natl. Acad. Sci. USA* **79**, 1558–62.

Thomson, T. & Lasko, P. (2005). Tudor and its domains: germ cell formation from a Tudor perspective. *Cell Res.* **15**, 281–91.

Villegas, J., Araya, P., Bustos-Obregon, E. & Burzio, L.O. (2002). Localization of the 16S mitochondrial rRNA in the nucleus of mammalian spermatogenic cells. *Mol. Hum. Reprod.* **8**, 977–83.

Volodina, N., Denegre, J.M. & Mowry, K.L. (2003). Apparent mitochondrial asymmetry in *Xenopus* eggs. *Dev. Dynam.* **226**, 654–62.